EurJIC

European Journal of Inorganic Chemistry

Chemistry Europe

European Chemical Societies Publishing

Accepted Article

Title: Tetrahedral Cu(I) complexes as electrocatalysts for the reduction of protons to dihydrogen gas

Authors: Wen Liang James Loke, Chen Hu, and Wai Yip Fan

To be cited as: *Eur. J. Inorg. Chem.* 10.1002/ejic.202100295

Link to VoR: https://doi.org/10.1002/ejic.202100295

WILEY-VCH

European Journal of Inorganic Chemistry 10.1002/ejic.202100295

Tetrahedral Cu(I) complexes as electrocatalysts for the reduction of protons to dihydrogen gas

Wen Liang James Loke[a], Chen Hu[a], and Wai Yip Fan*[a]

[a] Mr. W. L. J. Loke, Dr. C. Hu and Prof. W. Y. Fan
Department of Chemistry
National University of Singapore
3 Science Drive 3, Singapore 117543
E-mail: chmfanwy@nus.edu.sg

ABSTRACT: Four copper(I) complexes $[Cu(MeCN)_4]PF_6$ (**1**), $[Cu(dppe)_2]PF_6$ (**2**), $[Cu(bpy)_2]PF_6$ (**3**) and $[Cu(bpy)(dppe)]PF_6$ (**4**) have been used as electrocatalysts in the generation of dihydrogen from proton reduction. Low overpotentials of 0.4V have been measured using cyclic voltammetry when **1** and **3** were used as the catalysts in the presence of acetic acid as the proton source in acetonitrile. In contrast, a higher overpotential is observed for **4** while **2** is unable to catalyse the process. A mechanism for proton reduction has been proposed.

INTRODUCTION

The production of hydrogen from water, a cheap and abundant source, has been regarded as an ideal energy source to replace fossil fuels[1-3]. The proton reduction to hydrogen reaction which forms half of water splitting has thus become a focus of active research[4-5]. Although platinum is a highly efficient catalyst in water-splitting[6], its high cost prohibits large-scale hydrogen production. Therefore the search for lower-cost catalysts is still ongoing in order to achieve economical industrialization[7-9].

Many studies have focused on the [FeFe] and [NiFe] hydrogenases[10-12], a class of biological enzyme capable of releasing hydrogen from water reversibly and efficiently. These have resulted in the development of many mimics or model catalysts containing nickel and iron cores[13-14].

On the other hand, several non-biomimetic approaches which utilized different metal cores such as cobalt (Co)[15-18], copper (Cu)[19-21] and molybdenum (Mo)[22-23] have also been reported to display comparable catalytic activity as the hydrogenase models.

Surprisingly, copper-containing compounds have been one of the least-developed hydrogen evolution catalysts with the first molecular catalyst $[(bztpen)Cu(II)](BF_4)_2$ (bztpen = *N*-benzyl-*N*,*N'*,*N'*-tris(pyridin-2-ylmethyl)ethylenediamine) reported in 2014[19]. Since then, a few other copper(II) complexes containing nitrogen (N) and oxygen (O) donors[20-21] such as $Na_2[Cu(opba)]$ (opba: o-phenylenebis(oxamato)) and $[CuL^1](ClO_4)_2$ (L^1: 1,3-bis{[(1-methyl-1H-imidazol-2-yl)methyl]amino}propan-2-ol).

However, there have been much fewer reports of Cu (I) compounds acting as proton reduction catalysts or catalytic precursors. The use of $[Cu(pq)_2][BF_4]$ (pq : quinoxaline) as both photocatalyst and electrocatalyst has only recently been studied where reduction of trifluoroacetic acid was observed in dimethylformamide at an overpotential of 0.72V. Interestingly instead of the Cu(I) center, the pq ligand is proposed to be more heavily involved in the protonation and electrochemical reduction steps[24].

As most catalysts go through a reduction process during the catalytic cycle, we reason that Cu(II) compounds are likely to reduce to Cu(I) at some stage of the cycle. This has led us to prepare some Cu(I) complexes as the starting material so that their role in the hydrogen evolution process can be explored and evaluated.

In this work, we have used the commercially-available $[Cu(MeCN)_4]PF_6$ (**1**) as a precursor to synthesize three more Cu(I) complexes containing phosphine and nitrogen-centred ligands such as $[Cu(dppe)_2]PF_6$ (**2**), $[Cu(bpy)_2]PF_6$ (**3**) and a mixed copper N_2P_2 complex, $[Cu(bpy)(dppe)]PF_6$ (**4**). Cyclic voltammetry is then used to evaluate the efficiency of these four complexes as proton reduction electrocatalysts. How the various ligands affect the catalysis will be discussed and a proton reduction mechanism is proposed based on our experimental data.

RESULTS AND DISCUSSIONS

Preparation and Characterization of Complexes. The synthetic method for the complexes was modified from the process outlined by Min *et al.*[25] Complexes **2**-**4** were readily synthesized by direct coordination of the desired ligand to the Cu^I center of **1**. For each synthesis, two bidentate ligands displaced the weakly bounded acetonitrile ligands, forming a four-coordinated copper(I) complex. The structures of the complexes are shown in Scheme 1.

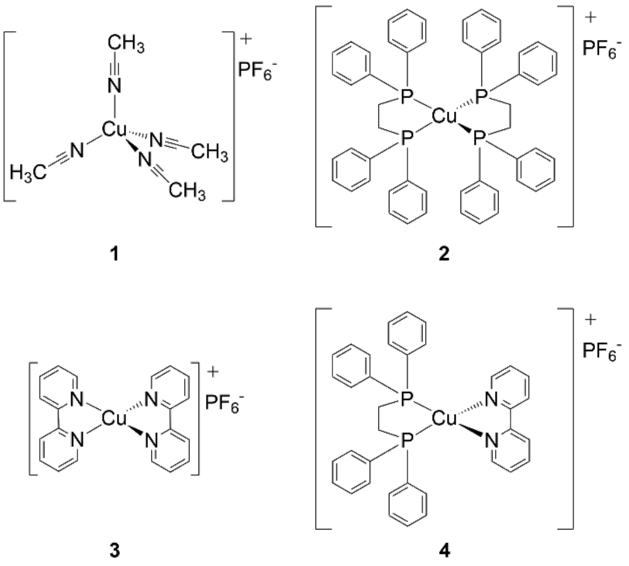

Scheme 1. Molecular structures of complexes **1**-**4**.

As coordinatively-saturated Cu(I) complexes, the products are relatively stable in the solid state and do not undergo disproportionation to Cu(0) and Cu(II) readily, a reaction common for a number of Cu(I) compounds[26-27]. However, a nitrogen atmosphere is still required during synthesis in order to prevent oxidation of Cu(I) and possibly the ligands.

The structures of **2**-**4** were identified through their ESI-MS, IR and NMR (^{1}H and/or ^{31}P) spectra (Supporting Information, S1-S11). Melting point determination were also carried out. In our experiment, we were able to isolate **3** as a reddish-brown solid. However, upon dissolution in chloroform for over two hours, the solution slowly changed from dark red to pale yellow, suggesting decomposition of **3**. Broad signals were thus observed in its NMR spectrum; this observation was also noted by Andrés-Tomé *et al.*[28] It is thus essential to use a freshly-prepared solution of **3** immediately for subsequent electrochemical studies.

Cyclic Voltammetry Studies. The cyclic voltammograms of the complexes **1**-**4** in acetonitrile were first recorded in the absence of acid using a glassy carbon working electrode (Figure 1). All solutions were freshly prepared and used immediately.

Complex **1** shows a reduction (cathodic) peak at around E_{pc} = -1.05 V (note that all potentials quoted herein are referenced against the ferrocene couple Fc^{+}/Fc in MeCN). The molecular reduction peaks for **2**, **3** and **4** were observed at E_{pc} = -1.40 V, E_{pc} = -1.19 V and E_{pc} = -1.47 V respectively. By comparison with the literature CV profiles[29] and the standard reduction potentials, the aforementioned reduction peaks have been assigned to the Cu^{I}/Cu^{0} couple of the respective complexes. A sharp oxidation (anodic) peak at -0.52 V was seen in the voltammograms of **1** and **3** together with another oxidation peak which appeared close to 0 V and superimposed on the Fc/Fc^{+} couple (indicated by the vertical dashed arrows). The oxidation peak at -0.52 V is attributed to the reverse process where elemental Cu(0) is oxidised to Cu(I) ions while the peak at 0 V belongs to the Cu^{I}/Cu^{II} couple.

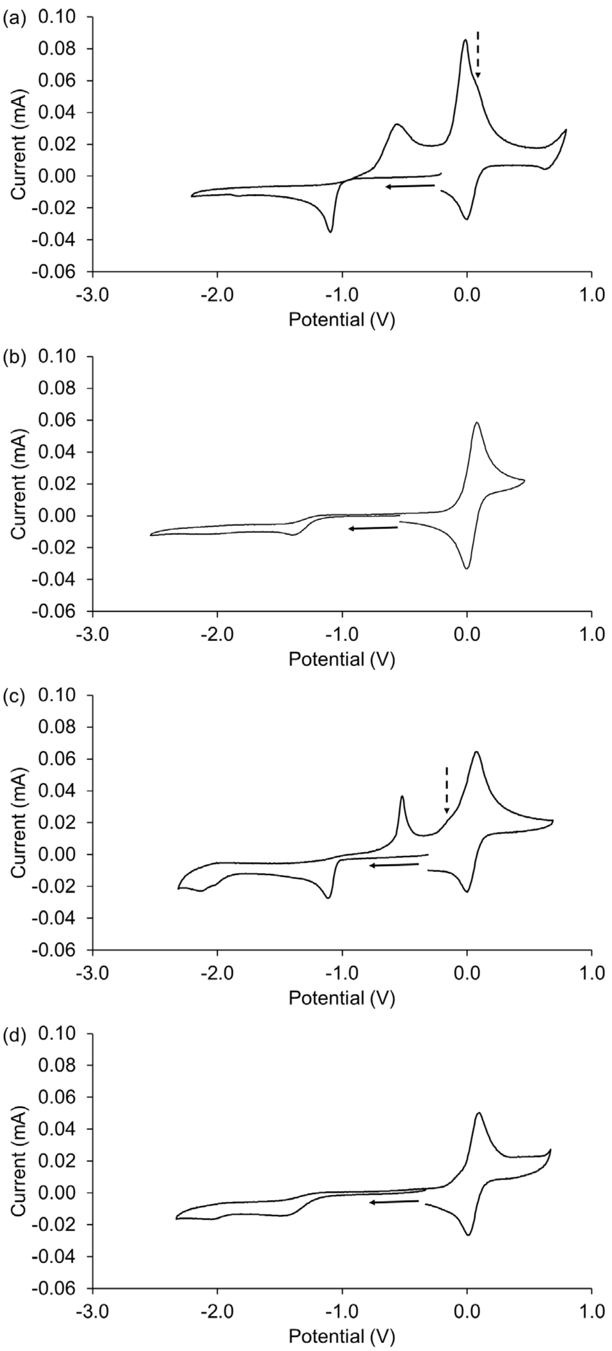

Figure 1. Cyclic voltammograms recorded of acetonitrile solutions containing 1 mM of the Cu(I) complex, 0.1 M $Bu_4N^{+}PF_6^{-}$ and 1 mM Fc at a scan rate of 100 mV/s. (a) **1** (b) **2** (c) **3** (d) **4**.

For **3** and **4**, we notice a second reduction wave occurring at a more negative potential of around -2.0 V. This wave most likely arises from the reduction of the bpy ligand[30], which is the common ligand for both complexes.

The assignment of the peaks has indicated the weakly-bound coordinating nature of acetonitrile (in **1**) and bpy ligands (in **3**). They have a tendency to dissociate from the copper centre after its initial reduction, hence leaving the generated elemental copper to be oxidized when the scan direction is reversed. The CV profiles also implied the relative stability for complexes containing dppe ligands (**2** and **4**), where elemental copper oxidation at -0.52 V was not observed.

The CV profiles of the complexes recorded in increasing amount of acetic acid were investigated next (Figure 2). For **1**, **3** and **4**, strong cathodic peaks appeared during the scan and continued to grow with increasing acid concentration. The acid-concentration dependence strongly suggests that catalytic reduction of protons is indeed occurring while the appearance of a peak shows that the process is diffusion-limited. However an acid-dependent wave was not observed for **2** (Figure 2b).

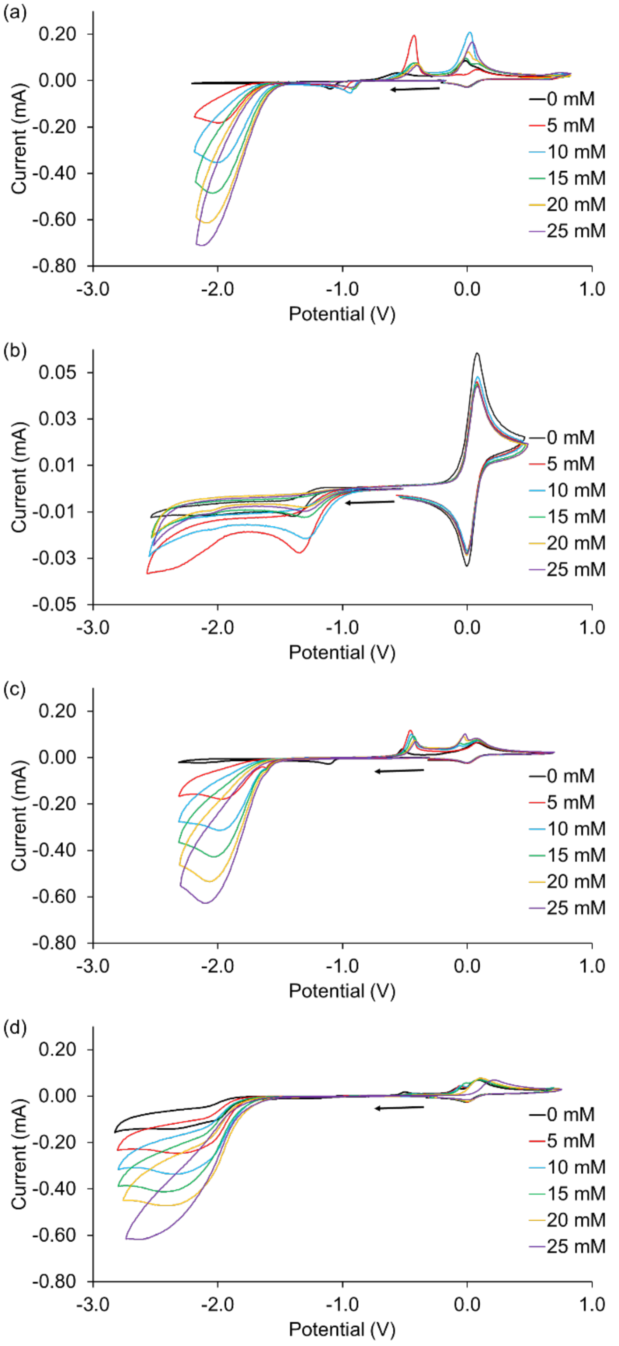

Figure 2. Cyclic voltammograms recorded of acetonitrile solutions containing 1 mM of the Cu(I) complex, 0.1 M $Bu_4N^+PF_6^-$ and 1 mM Fc at a scan rate of 100 mV/s with increasing acetic acid concentration from 0 mM to 25 mM. (a) **1** (b) **2** (c) **3** (d) **4**.

Apart from the appearance of the catalytic wave, there was a change in the oxidation peaks at -0.52 V and at 0 V with varying acetic acid concentrations (See Supporting Information Figure S12 for an enlarged version of Figure 2). For **1** and **3**, the current at -0.52 V decreases with an increasing amount of acid. In contrast the oxidation peak at 0 V grows in intensity. It would appear that Cu(0) generation is less favoured compared to Cu(I) under high acid conditions. These peaks were also observed to a smaller extent for **4** but did not appear for **2**. The change in the peak intensities of these oxidation processes will provide some useful information for understanding the mechanism later.

To evaluate the activity of the copper catalysts, we have determined their overpotential necessary for catalysis, which can be expressed by the following equation[31]

$$\text{Overpotential necessary for catalysis} = \left|E_{cat/2} - E^{o}_{\mathrm{HA}}\right|$$

where $E_{cat/2}$ is the catalytic half-wave potential and

$$E^{o}_{\mathrm{HA}} = E^{o}_{\mathrm{H^+}} - \left(\frac{2.303RT}{F}\right)\mathrm{p}K_{\mathrm{a,HA}}$$

Using the values $E^{\mathrm{o}}_{\mathrm{H^+}}$ = -0.028 V[29] and $\mathrm{p}K_{\mathrm{a,AcOH}}$ = 22.3[32], the thermodynamic potential $E^{\mathrm{o}}_{\mathrm{AcOH}}$ is calculated to be -1.35 V. With the catalytic half-wave potential determined using the method of Appel and Helm[33], the overpotential necessary for catalysis of the complexes (Table 1) were computed by the following,

$$\text{Overpotential necessary for catalysis} = \left|E_{cat/2} + 1.35\right| \ (\mathrm{V})$$

Table 1. Electrochemical data for complexes **1-4**. [a]Based on peak current value at 15 mM acetic acid and 1 mM of complex. [b]Values obtained from bulk electrolysis experiments. N.D. = not determined.

Complex	1	2	3	4
Reduction Peak Potential for Cu^I/Cu^0 (V)	-1.05	-1.40	-1.19	-1.47
Catalytic Half-wave Potential[a], $E_{cat/2}$ (V)	-1.77	N.D.	-1.78	-1.94
Overpotential necessary for catalysis[a] (V)	0.43	N.D.	0.44	0.60
Turnover Number, TON[b]	19.7 ± 3.9	N.D.	15.3 ± 2.4	12.8 ± 2.9

The use of **1** or **3** as the catalyst resulted in the lowest overpotential (0.4 V) for proton reduction, which compares favourably with some of the best mimics of hydrogenases[7,8]. In addition, their molecular reduction peaks occur at a more positive potential relative to the thermodynamic potential (-

1.35 V) of acetic acid reduction in acetonitrile. Somehow the ease of molecular reduction may have facilitated the subsequent proton reduction process to take place at a much lower overpotential. Complexes **1** and **3** also have very similar overpotentials. This observation suggests that a common intermediate species may have been generated upon dissociation of the acetonitrile and bpy ligands in **1** and **3** respectively.

In contrast, **2** did not exhibit catalytic behaviour while **4** gave rise to a higher overpotential compare to **1** and **3**. The inactivity of **2** could be due to the tightly-bound dppe ligand preventing the interaction of the Cu core with acetic acid or protons. The stability of **2** is also supported by its partial electrochemical reversibility depicted in Figure 2. While complex **4** also contains dppe, dissociation of the bpy ligand would still be able to provide a vacant site for proton interaction.

We have conducted control experiments in the absence of the copper complexes and noted only small contributions from the direct reduction of acetic acid at the electrode surface (Supporting Information, Figure S13). Thus the current generated at the respective $E_{cat/2}$ potential of each catalyst was mostly derived from the proton reduction process driven by the catalyst itself.

Bulk electrolysis experiments have been conducted for **1**, **3** and **4** for several hours in large excess (1000 equiv.) of acetic acid. Dihydrogen gas was successfully detected in the headspace using mass spectrometry. From the chronoamperometry profiles (Supporting Information, Figures S14-S16), the TON (Turnover Number) for each catalyst has been estimated and shown in Table 1.

Rinse test has also been carried out to shed more light into the proton reduction mechanism (Supporting Information, Figure S17). For each test, the electrodes were first immersed into a solution containing the catalyst and a fixed equivalent of acid. After ten cycles of CV scans, the electrodes were removed from the solution and rinsed with acetonitrile. They were re-immersed into a fresh acetonitrile solution containing only acetic acid (without any copper catalyst) and CV scans were recorded thereafter. It was found that none of the new CV profiles registered proton reduction signals. This set of experiments indicates that there is no significant amount of catalyst deposited on the electrode surface. However it still does not rule out contributions from highly-active heterogeneous species which requires only a small amount for catalysis.

Proposed Mechanism. The proton reduction mechanism consists of two electrochemical (E) and two chemical (C) or protonation steps undertaken by the catalyst. We are interested in determining the sequence of these steps for **1** and **3** as they have been shown to be the more efficient catalysts (Figure 3). UV-visible absorption experiments were carried out in order to verify whether these catalysts undergo protonation, which will lead to a change in absorbance, prior to electrochemical reduction. For each complex dissolved in acetonitrile, the UV spectrum before and after the addition of acetic acid did not show any peak shift or significant intensity changes despite adding excess acid (Supporting Information, Figures S18-S21). Therefore initial protonation of the complexes does not occur or it is too slow to be considered the first step in the mechanism.

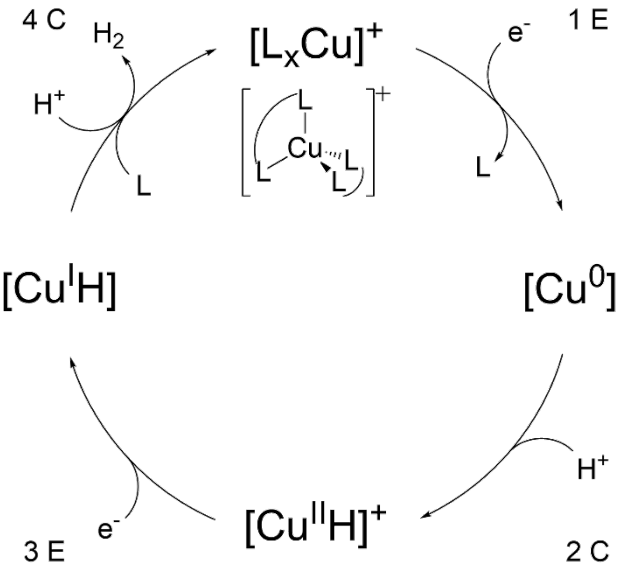

Figure 3. Proposed mechanism for proton reduction catalysed by the Cu(I) complexes. L represents the ligand surrounding the copper centre. The steps are numbered according to the sequence (1 to 4) and whether they are electrochemical (E) or chemical protonation (C).

The results above lead us to propose the molecular reduction peak observed in the CV scan to be the first electrochemical step. It is interesting to speculate on the nature of the Cu(0) species generated upon reduction. Cu(0) complexes are rarely stable; most of the known complexes[34-38] are highly air- and moisture-sensitive and difficult to isolate. It is highly unlikely that such a stable Cu(0) complex can be generated under our experimental conditions. As mentioned, the similarity in the overpotential values exhibited by **1** and **3** suggests that their electrochemical reduction probably lead to ligand dissociation and subsequent deposition of elemental copper on the electrode surface. Furthermore the observation of a significant Cu(0) to to Cu(I) oxidation peak at -0.52V for **1** and **3** supports the hypothesis. In contrast, the phosphine ligands of **2** and **4** may have retained its coordination to Cu^0 on the surface sufficiently long to disrupt the catalytic cycle.

The second step of the mechanism is very likely a protonation step (C) as a subsequent electrochemical step would have generated copper with an oxidation state of -1. As noted earlier, we have observed a decrease in the Cu^0/Cu^I oxidation peak at -0.52 V with increasing acid concentration (see Figure 3). This observation could be explained if the increase in the acid concentration accelerates the protonation of Cu(0) on the surface leading to the formation of a cationic Cu(II)-H hydride species. If this formation is followed by a one-electron reduction as the third step, a neutral Cu(I) hydride species will be produced. However it is also likely that the second and third steps are combined to form a proton-coupled electron transfer step[39], a process common in electrochemical reactions. For example, slow protonation in step 2 will hamper the catalytic process but once coupled with an exergonic electron transfer, catalysis can proceed at a more facile rate.

Some evidence supporting the presence of an active but relatively long-lived copper intermediate is presented when the CV experiments at varying scan rates (Figure 4) were performed. The CV recorded (black line) for the precursor complex with 15 equivalents of acetic acid showed curve crossing occurring at a low scan rate of 10 mV s^{-1}. The presence of curve crossing indicates the generation of intermediate copper species with redox couples more positive than the reactant redox couple. In our experiments, this intermediate would correspond to the proposed Cu(I) hydride complex. As the current did not return to near-zero on the anodic scan, some catalytic activity for the species is still observed even though the local concentration of substrate was reduced during the forward scan catalysis. Curve crossing may also suggest an ECE mechanism[40], which is consistent with the reaction pathways so far.

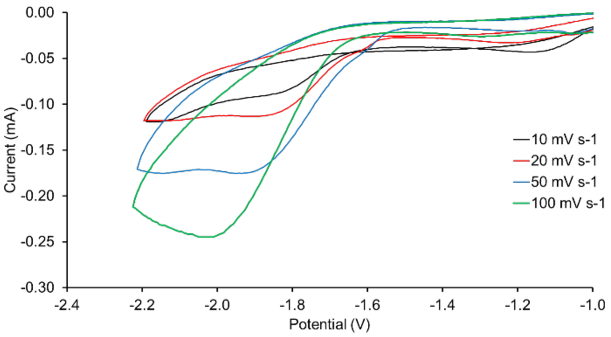

Figure 4. Cyclic voltammograms recorded of acetonitrile solutions containing 1 mM of **1**, 0.1 M Bu_4NPF_6, 1 mM Fc and 15 mM AcOH at different scan rates. Curve crossing (black line) is observed when the scan rate is lowered to 10 mV s^{-1}.

In the fourth step, the Cu(I) hydride species couples with a proton to release dihydrogen gas and regenerates the Cu(I) cation complex. Therefore we propose an ECEC mechanism for complexes **1** and **3** acting as proton reduction catalysts. We believed that this mechanism may also be applicable for **2** and **4** where the phosphine ligands have deactivated the Cu(0) species on the electrode surface and thus impeded the catalytic cycle. Further work is being planned to understand the roles played by strong donor ligands in Cu(I)-catalysed proton reduction processes.

EXPERIMENTAL SECTION

Chemicals. Tetrakis(acetonitrile)copper(I) hexafluorophosphate $[Cu(MeCN)_4]PF_6$, 2,2'-bipyridyl (bpy), 1,2-bis(diphenylphosphino)ethane (dppe), tetrabutylammonium hexafluorophosphate $Bu_4N^+PF_6^-$ were purchased from Aldrich. Ferrocene (Fc) was purchased from Riedel-de Haën. Solvents such as dichloromethane (DCM) were purchased from Fisher Chemical, while acetonitrile (MeCN) was purchased from Fulltime and diethyl ether (Et_2O) was purchased from J.T.Baker. Deuterated solvents such as chloroform-*d* ($CDCl_3$) were purchased from Cambridge Isotope Laboratories. All chemicals and solvents purchased were used directly without purification.

General Procedures. All synthetic procedures were carried out under inert N_2 conditions. Melting points were determined using OptiMelt MPA100 Melting Point Apparatus. Electrospray ionization mass spectrometry (ESI-MS) was conducted using a Finnigan MAT LCQ spectrometer. Fourier Transform Infrared (FT-IR) spectra were acquired with solid samples in KBr disk using Bruker Alpha FT-IR spectrometer. ^1H NMR and ^{31}P NMR were recorded using Bruker ACF500 NMR spectrometer at room temperature.

Electrochemical Experiments. All electrochemical experiments were conducted at 298 (±2) K. (a) Cyclic voltammetry experiments were conducted with a computer-controlled potentiostat (Princeton Applied Research Potentiostat Model 263A) using a three-electrode system. The working electrode was a 3 mm-diameter planar glassy carbon (GC) disk, used together with a platinum counter electrode and a silver wire miniature reference electrode connected to the test solution via a salt bridge (containing 0.5 M Bu_4NPF_6 in MeCN). Prior to each scan, the solutions used for voltammetric analysis were purged with high purity nitrogen gas, and the working electrodes were prepared by polishing with an alumina oxide (grain size 0.3 μm) slurry on a Buehler Ultrapad polishing cloth, rinsing with ultrapure water and acetone, and then drying. The test solutions were comprised of 1 mM analyte and 0.1 M supporting electrolyte ($Bu_4N^+PF_6^-$) in MeCN. Accurate potentials were obtained by using ferrocene (Fc) as an internal standard. (b) Bulk electrolysis was conducted with sample solutions containing 1 mM analyte, 1 M acetic acid in 0.1 M $Bu_4N^+PF_6^-$ in MeCN. The sample solutions were electrolyzed at the respective catalytic peak potential. The chronoamperometry curve was generated. The gaseous content of the reaction vessel was removed with a syringe of 1 cm^3 volume and injected into a mass spectrometer tuned to m/z = 2, corresponding to the detection of H_2.

Syntheses of the Copper Complexes. $[Cu(MeCN)_4]PF_6$ (74.4 mg, 0.2 mmol) was dissolved in DCM (1 mL) under nitrogen flow. The corresponding ligand was dissolved in DCM (1 mL) and the resultant solution was added dropwise to the copper solution. An immediate color change from the original colorless solution was observed. The mixture was allowed to stir for 30 minutes. The solid product was precipitated by the addition of diethyl ether to the reaction mixture, and was collected via suction filtration.

$[Cu(dppe)_2]PF_6$ (2). dppe (159.2 mg, 0.4 mmol) was used as the ligand. White solid was obtained following the general procedure outlined above. Yield: 132.2 mg, 66% (based on $[Cu(MeCN)_4]PF_6$). mp 233 °C. Anal. Calcd for $C_{52}H_{48}P_5F_6Cu$:

C, 62.12; H, 4.82. Found: C, 61.72; H, 5.22. ESI-MS (DCM, +, m/z): 859 ([Cu(dppe)$_2$]$^+$). ^{1}H NMR (CDCl$_3$, 500 MHz, δ): 2.39 (d, 8H, CH$_2$), 7.04-7.76 (m, 40H, Ph). ^{31}P NMR (CD$_3$CN, 500 MHz, δ): -144.63 (m, PF$_6^-$), 6.35 (br, dppe).

[Cu(bpy)$_2$]PF$_6$ (3). bpy (62.4 mg, 0.4 mmol) was used as the ligand. Reddish-brown solid was obtained following the general procedure outlined above. Yield: 89.1 mg, 86% (based on [Cu(MeCN)$_4$]PF$_6$). mp 239 °C. Anal. Calcd for $C_{20}H_{16}N_4PF_6Cu$: C, 46.11; H, 3.10; N, 10.76. Found: C, 45.58; H, 2.88; N, 11.30. ESI-MS (DCM, +, m/z): 375 ([Cu(bpy)$_2$]$^+$). ^{1}H NMR (CDCl$_3$, 500 MHz, δ): 7.56 (s, 4H), 8.10 (br, 4H), 8.44 (br, 8H).

[Cu(bpy)(dppe)]PF$_6$ (4). dppe (79.6 mg, 0.2 mmol) and bpy (31.2 mg, 0.2 mmol) were used as the ligands. Yellow solid was obtained following the general procedure outlined above. Yield: 140.8 mg, 93% (based on [Cu(MeCN)$_4$]PF$_6$). mp 235 °C. Anal. Calcd for $C_{36}H_{32}N_2P_3F_6Cu$: C, 56.65; H, 4.24; N, 3.67. Found: C, 57.08; H, 4.24; N, 3.43. ESI-MS (DCM, +, m/z): 617 ([Cu(bpy)(dppe)]$^+$). ^{1}H NMR (CDCl$_3$, 500 MHz, δ): 2.64 (dd, 4H, CH$_2$), 7.14-7.44 (m, 20H, Ph), 7.49 (dd, 2H, bpy), 8.17 (dd, 2H, bpy), 8.32 (d, 2H, bpy), 8.56 (d, 2H, bpy). ^{31}P NMR (CD$_3$CN, 500 MHz, δ): -144.63 (m, PF$_6^-$), -5.20 (br, dppe).

ASSOCIATED CONTENT

Supporting Information. This material is available free of charge via the Internet at http://pubs.acs.org.

AUTHOR INFORMATION

Corresponding Author

*E-mail for W.Y.F.: chmfanwy@nus.edu.sg.

ACKNOWLEDGMENT

We acknowledge the National University of Singapore for participating through a research grant 143-000-B49-114.

Keywords: Proton reduction • copper • electrochemistry • mechanism • green chemistry

REFERENCES

1. G. W. Crabtree, M. S. Dresselhaus, M. V. Buchanan, *Phys. Today* **2004**, *57*, 39-44.
2. S. S. Penner, *Energy* **2006**, *31*, 33-43.
3. S. Chu, Y. Cui, N. Liu, *Nat. Mater.* **2016**, *16*, 16-22.
4. M. Wang, Z. Wang, X. Gong, Z. Guo, *Renew. Sustain. Energy Rev.* **2014**, *29*, 573-588.
5. B. You, Y. Sun, *Acc. Chem. Res.* **2018**, *51*, 1571-1580.
6. S. M. Haile, *Acta Mater.* **2003**, *51*, 5981-6000.
7. M. Wang, L. Chen, L. Sun, *Energy Environ. Sci.* **2012**, *5*, 6763-6778.
8. J. R. McKone, S. C. Marinescu, B. S. Brunschwig, J. R. Winkler, H. B. Gray, *Chem. Sci.* **2014**, *5*, 865-878.
9. X. Zou, Y. Zhang, *Chem. Soc. Rev.* **2015**, *44*, 5148-5180.
10. P. M. Vignais, B. Billoud, *Chem. Rev.* **2007**, *107*, 4206-4272.
11. W. Lubitz, H. Ogata, O. Rüdiger, E. Reijerse, *Chem. Rev.* **2014**, *114*, 4081-4148.
12. D. Brazzolotto, M. Gennari, N. Queyriaux, T. R. Simmons, J. Pécaut, S. Demeshko, F. Meyer, M. Orio, V. Artero, C. Duboc, *Nat. Chem.* **2016**, *8*, 1054-1060.
13. C. Tard, C. J. Pickett, *Chem. Rev.* **2009**, *109*, 2245-2274.
14. F. Gloaguen, T. B. Rauchfuss, *Chem. Soc. Rev.* **2009**, *38*, 100-108.
15. X. Hu, B. M. Cossairt, B. S. Brunschwig, N. S. Lewis, J. C. Peters, *Chem Commun* **2005**, 4723-4725.
16. G. M. Jacobsen, J. Y. Yang, B. Twamley, A. D. Wilson, R. M. Bullock, M. R. DuBois, M.; D. L. DuBois, *Energy & Environ. Sci.* **2008**, *1*, 167-174
17. P. A. Jacques, V. Artero, J. Pécaut, M. Fontecave, *Proc. Nat. Acad. Sci.* **2009**, *106*, 20627-20632.
18. J. P. Bigi, T. E. Hanna, W. H. Harman, A. Chang, C. J. Chang, *Chem Commun* **2010**, *46*, 958-960.
19. P. Zhang, M. Wang, Y. Yang, T. Yao, L. Sun, *Angew. Chem. Int. Ed..* **2014**, *53*, 13803-13807.
20. L. Z. Fu, T. Fang, L. L. Zhou, S. Z. Zhan, *RSC Adv.* **2014**, *4*, 53674-53680.
21. S. Nestke, M. Kügler, J. Scholz, M. Wilken, C. Jooss, I. Siewert, *Eur. J. Inorg. Chem.* **2017**, *2017*, 3376-3382.
22. H. I. Karunadasa, C. J. Chang, J. R. Long, *Nature* **2010**, *464*, 1329-33.
23. H. I. Karunadasa, E. Montalvo, Y. Sun, M. Majda, J. R. Long, C. J. Chang, *Science* **2012**, *335*, 698-702.
24. M. Drosou, F. Kamatsos, G. Ioannidis, A. Zarkadoulas, C. A. Mitsopoulou, C. Papatriantafyllopoulou, D. Tzeli, *Catalysts* **2020**, *10*, 1302-1315.
25. J. Min, Q. Zhang, W. Sun, Y. Cheng, L. Wang, *Dalton Trans.* **2011**, *40*, 686-93.
26. F. Fenwick, *J. Am. Chem. Soc* **1926**, *48*, 860-870.
27. E. Solari, M. Latronico, P. Blech, C. Floriani, A. Chiesi-Villa, C. Rizzoli, *Inorg. Chem.* **1996**, *35*, 4526-4528.
28. I. Andres-Tome, J. Fyson, F. B. Dias, A. P. Monkman, G. Iacobellis, P. Coppo, *Dalton Trans.* **2012**, *41*, 8669-74.
29. M. J. Samide, D. G. Peters, *J. Electroanal. Chem.* **1998**, *443*, 95-102.
30. S. Roffia, M. Marcaccio, C. Paradisi, F. Paolucci, V. Balzani, G. Denti, S. Serroni, S. Campagna, *Inorg. Chem.* **1993**, *32*, 3003-3009.
31. E. S. Rountree, B. D. McCarthy, T. T. Eisenhart, J. L. Dempsey, *Inorg. Chem.* **2014**, *53*, 9983-10002.
32. V. Fourmond, P. A. Jacques, M. Fontecave, V. Artero, *Inorg. Chem.* **2010**, *49*, 10338–10347.

33. A. M. Appel, M. L. Helm, *ACS Catal.* **2014**, *4*, 630-633.
34. D. S. Weinberger, N. Amin Sk, K. C. Mondal, M. Melaimi, G. Bertrand, A. C. Stuckl, H. W. Roesky, B. Dittrich, S. Demeshko, B. Schwederski, W. Kaim, P. Jerabek, G. Frenking, *J. Am. Chem. Soc.* **2014**, *136*, 6235-6238.
35. G. W. Watt, J. W. Dawes, *J. Inorg. Nucl. Chem.* **1960**, *14*, 32-34.
36. H. Huber, D. McIntosh, G. A. Ozin, *J. Organomet. Chem.* **1976**, *112*, C50-C54.
37. G. A. Bowmaker, *Aust. J. Chem.* **1978**, *31*, 2549-2553.
38. P. H. Kasai, P. M. Jones, *J. Am. Chem. Soc.* **1985**, *107*, 813-818.
39. C. Costentin, M. Robert, J-M. Savéant, *J. Am. Chem. Soc.* **2006**, *128*, 4552–4553.
40. M. A. Fox, R. J. Akaba, J. *Am. Chem. Soc.* **1983**, *105*, 3460-3463.

10.1002/ejic.202100295

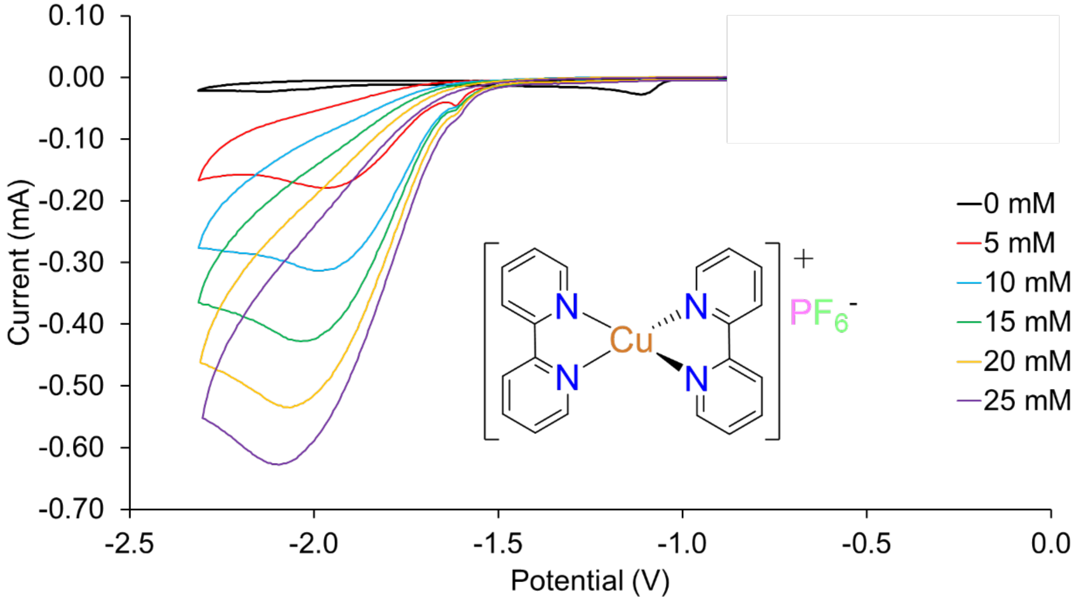

For Table of Contents Only

Table of Contents Synopsis:

Cu (I) complexes have been demonstrated to be efficient proton reduction electrocatalysts in acetonitrile. An overpotential value approaching 0.4V has been achieved for $Cu(CH_3CN)_4^+PF_6^-$ using acetic acid as the proton source. Adsorbed Cu atoms generated from the reduction of Cu(I) are believed to play a vital role in the catalytic cycle.